Design and development of a dexterous teleoperation setup for nuclear waste remote manipulation

Florian Gosselin, Mathieu Grossard

Design and development of a dexterous teleoperation setup for nuclear waste remote manipulation

Florian Gosselin[1][0000-0003-3412-8144], Mathieu Grossard[1]

[1] Université Paris-Saclay, CEA, LIST, F-91120 Palaiseau, France
florian.gosselin@cea.fr

Abstract. Teleoperation is entering a new era. Despite still in use today in the nuclear industry, simple purely mechanical or robotic 6 degrees of freedom (DoF) master-slave systems equipped with bi-digital grippers on the slave side and simple handles on the master side are not able to answer the challenge of remote manipulation at scale. These historical remotely controlled robotic solutions, inherited from mechanical master slave systems developed decades ago for research activities performed in gloveboxes and hot cells, allow operators an efficient and safe access to dangerous materials at distance. They are adapted when the variety of the to-be-manipulated objects remains limited, especially when these objects can be adapted for remote manipulation. They are however no more sufficient when one has to handle a much higher quantity of much more diverse objects, as it is typically the case when processing nuclear waste accumulated in huge quantities over time and/or produced at the occasion of nuclear power plants' dismantling operations. The quantity and diversity of nuclear waste require more efficient and versatile systems. To answer this challenge and increase the operators' productivity, we developed a complete bimanual teleoperation setup able to perform remote dexterous manipulation tasks. This article describes the hardware and software architecture of this platform, which is notably composed of a novel dexterous master-slave system combining a tri-digital master glove and a remotely controlled three fingers gripper. Both make use of highly backdrivable actuators and transmissions, and the proposed coupling schemes allow intuitive control of various grasp types. As a result, the proposed setup enables dexterous and force-sensitive control, and it is well-suited for high fidelity force-reflection tele-presence.

Keywords: Teleoperation, Dexterous manipulation, Multi-finger gripper, Hand exoskeleton, Force Feedback.

1 Introduction

The rise of the nuclear industry in the middle of the twentieth century required the development of efficient processes allowing to handle radioactive material without exposing operators to danger. The solution found by researchers and engineers to grasp and manipulate radioactive objects in laboratory settings was to use remote manipulation means, among which telemanipulators are the most advanced and efficient solutions, to access safely dangerous materials disposed in gloveboxes and hot cells. The

objects themselves, in limited number, were adapted for remote manipulation, allowing their grasping and manipulation with simple 6 DoF master-slave systems equipped with bi-digital grippers. Various systems of this kind, being either purely mechanical of robotic devices, were developed and used over years in nuclear installations [1] [2]. They prove to be very efficient, especially those benefiting from computer assisted telemanipulation functions, and are still in use today, for example in the recycling plant of La Hague in France [3] [4].

Such solutions are however not able to answer the challenge of remote manipulation at scale. They were perfectly adapted for handling few radioactive objects, but they are no more sufficient when one has to handle a high quantity of very various objects, as it is typically the case when processing nuclear waste accumulated in huge quantities over the years of exploitation of nuclear power plants and/or produced at the occasion of their dismantling. The quantity and diversity of nuclear waste materials require more efficient and versatile systems. The objective of the RoMaNS (i.e. Robotic Manipulation for Nuclear Sort and Segregation) project, financed by the European Horizon 2020 research program, was to develop novel solutions able to answer this challenge [5] [6]. To better understand the problem, it can be recalled that only highly irradiated material must be stored in high-level storage containers and facilities which are extremely expensive and resource intensive. On the contrary, low level waste can be placed in low-level storage containers. In practice however, waste of mixed contamination levels were sometimes put together in storage containers, especially in the older nuclear sites (some dates back to the 1940s). It is now time to clean up this waste stock and develop a more sustainable solution to store each waste item in an adequate container. The vast quantities of legacy nuclear waste (in the UK for example, intermediate level waste amount to about 1.4 million cubic meters [7]) makes it critical to advance the state of the art in telemanipulation in order to solve the safety-critical industrial problem of sorting and segregating irradiated material.

This sorting process requires opening thousands of legacy waste containers, extracting their potentially very various contents (pieces of fuel rod casing, contaminated tools and rubble, irradiated suits, rubber gloves, etc.), and sorting and segregating the most highly contaminated objects. The high level of radiations of some waste material prevents manual operation, and the process can only be performed using remotely controlled robots. As previously explained, state-of-the-art 6 DoF master-slave systems equipped with bi-digital grippers are not a viable solution therefore in the longterm due to some important limitations. First, they do not allow grasping all kinds of objects being present in the containers. Also, they must be under permanent direct control of human operators, with poor productivity. The aim of the ROMANS project was to develop more dexterous and versatile telemanipulation means and mixed autonomy solutions allowing to answer these limits.

This paper, which is an extended version of the work presented in [8], addresses the first issue. Compared to [8], which focused on the master hand device, this article introduces additional information on the whole bi-manual teleoperation platform fitted for waste processing, with details on the slave hand and dexterous master-slave coupling schemes. It is organized as follows: section 2 first shortly introduces the whole platform, then section 3 and 4 present the dexterous slave gripper and the master hand device. Sections 5 and 6 give details on the coupling schemes used to control the system and introduce the first validation tests, and section 7 concludes the paper.

2 Bi-manual teleoperation platform

Figure 1 illustrates the bi-manual teleoperation set-up. This platform is composed of two slave robots in order to allow for a natural operation with both hands, a Stäubli RX160 equipped with a dexterous gripper and a prototype cobot developed at CEA equipped with a classical bi-digital gripper. These robots are controlled using two input devices mapping the slave-arm capabilities. A first Virtuose 6D TAO (www.haption.com) equipped with our novel hand master glove is used for the control of the first robot, allowing fine control of the dexterous gripper with force feedback on both the palm and fingers, and a second Virtuose 6D TAO equipped with a handle is used to control the second robot.

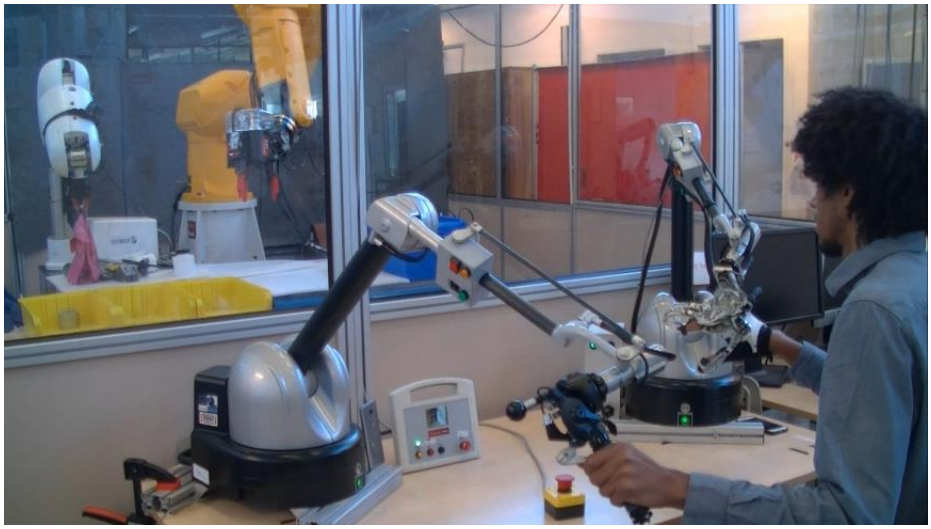

Fig. 1. Bi-manual dexterous teleoperation set-up (source [8]).

It is worth noting that to efficiently perform dexterous operations, the human beings often make use of both hands. This configuration allows some level of parallelization, and most importantly to concurrently perform complementary operations (e.g. holding a container with one hand and opening the lid with the second hand, opening a container and grasping an object inside it, grasping an object and making an operation on it, etc.). This configuration was used here, with one robot carrying a simple gripper used for rough operations, and the second one equipped with the three fingers gripper allowing to perform more dexterous tasks.

All components of this platform share a high backdrivability obtained either by design (esp. regarding actuators and transmissions) for the master arms, dexterous master glove and slave hand, and cobot prototype, or using a force/torque sensor for the Stäubli robot. As a result, both robots enable teleoperation with high fidelity force-reflection, thus intuitive and efficient remote operation. Further details on the slave and master hands are given below.

3 Dexterous three fingers gripper

3.1 Design rationales and principles

Human operators prove to be very efficient for waste sorting, comfort and safety issues aside. Their large experience of handling various objects in the daily life associated with the formidable flexibility, dexterity and sensitivity of the human hand, allows them to quickly adapt to any situation. The human hand has thus been an important source of inspiration for the design of dexterous multi-fingered robotic grippers like for example the Shadow Robot hand [9] [10], the anthropomorphic CEA-LIST hand [11] or the DLR AWIWI hand [12]. Some of these devices are natively backdrivable, allowing to estimate the grasping forces without additional force or torque sensors, while others make use of tendon tension sensors, force/torque sensors or tactile sensors therefore. Such grippers are capable of reproducing grasps found in usual grasping taxonomies [13] [14] and they allow performing dexterous tasks under direct human control in telerobotics with force feedback [15]. Their design, as well as their control, are however very complex and they remain in practice limited to laboratory experiments. None of them reached industrial settings and teleoperation slave arms and industrial robots still most often make use of simple bi-digital grippers or dedicated tools which in turn suffer a poor versatility.

A compromise between these two extremes is necessary to overcome this situation. As the most bulky and heavy components in a robot gripper are its actuators, a logical solution is to reduce their number. This can be done in two ways that we combine here:

- First, the number of fingers can be reduced. As we focus here on grasping, a configuration with three fingers is sufficient (should we have also targeted manipulation, a fourth finger as on the ROBIOSS hand [16] or additional embedded actuation means as in [17] would have been necessary). Yet to better adapt the gripper's configuration to the shape of the grasped objects and improve stability, a reconfigurable palm as present for example in the BarretHand [18] is implemented.
- Second, the gripper can be under-actuated, with coupling rods allowing to synchronize several degrees of freedom and springs allowing to passively adapt to the grasped objects' geometry as proposed in [19] and [20].

3.2 Electro-mechanical design

The three-fingers robotic gripper is illustrated in figure 2. Following the above-mentioned principles, this hand is composed of three fingers, one of which is fixed and the other two being mobile in abduction-adduction so as to allow cylindrical grasps when the adduction is null, spherical grasps around the center of the abduction-adduction range of motion and planar grasps when fingers are fully adducted (see figure 5 in section 3.4 below). Delrin gears actuated by a single motor (hidden in figure 2) allow coupling the abduction-adduction movements of the mobile fingers and the palm facing the fingers is slightly curved to favor the stability of the grasps once the objects are held in the gripper.

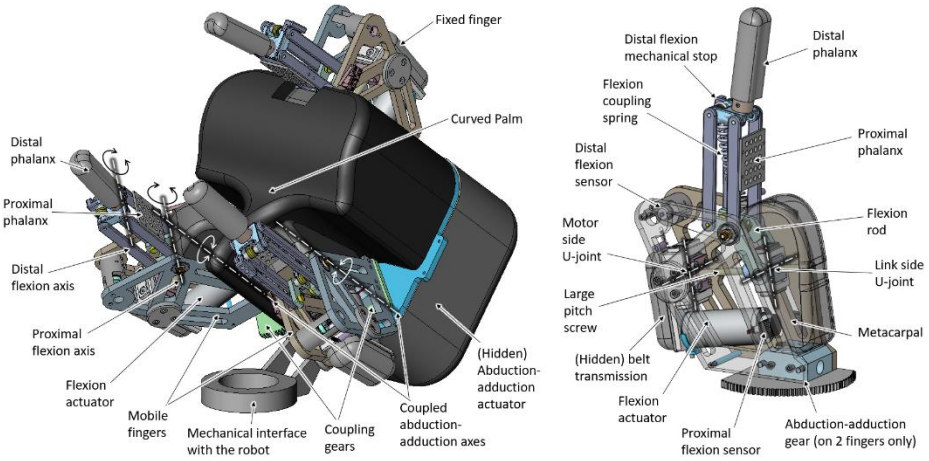

Fig. 2. Overview of CEA LIST's three fingers slave hand.

All three fingers have similar kinematics above the abduction-adduction axis. They are composed of a first link equivalent to human metacarpals, a proximal and a distal phalange. The fingers are underactuated, i.e. there is only one actuator controlling the two flexion DoFs. The actuation system is composed of a Maxon DCX26L DC motor (48V, continuous torque 59.1mNm, peak torque 697mNm [21]) associated with a belt transmission (reduction ratio equal to 1) driving a highly backdriveable ball screw (neutral diameter 5mm, pitch 2mm) which itself drives a nut undergoing a translation movement. At the output of the system, the nut drives a rod disposed at the base of the proximal phalange. The principle is the same as in Screw Cable Systems [22], except a direct transmission without any cable is used here. This solution has the advantage of a higher efficiency, at the price of a non constant reduction ratio as the lever arm between the driving screw-nut system and the moving rod axis varies as the finger moves in flexion. The finger itself is composed of two phalanges whose movements are coupled with a four bar mechanism and a spring. As long as there is no contact on the proximal phalange, the finger remains straight. The distal phalanx bends only when a contact occurs on the proximal phalanx, with a triggering force regulated by the four bar geometry and the spring characteristics (this force is equal to 30N here). One benefit of underactuation is that it allows both precision grasps when the object is contacted with the distal phalanges and power grasps of various objects when the contact first occurs on the proximal phalanges. In the latter case, the grasping movement has two phases: a sweeping phase, where the proximal links contact the object, and a caging phase, where the distal links make contact to fully enclose the object. It is worth noting that if contact on any finger is obstructed, the others continue to move, until the hand fully envelopes the object in a power grasp. Underactuation (both within the individual fingers and between the fingers) is thus favorable for achieving form closure as it can aid in maximizing the grasp contact surfaces. Moreover, all fingers are provided with interchangeable pads that can be attached on the proximal and distal phalanges so as to adapt the grasps form factor and the friction coefficient. Owing to the specifications of the different components, the continuous force in the nut can be estimated at about 167N with an hypothesis of a 90% efficiency (i.e. peak force 1970N). This corresponds to a theoretical flexion

torque equal to 4.9Nm continuous and 58Nm peak and a maximum force of about 33N continuous and 387N peak at the fingertip when the finger is fully extended and normal to the palm as shown in figure 2 (lever arm equal to 29.5mm, distance between the flexion rod axis and the fingertip equal to about 150mm).

The principle is the same on the abduction-adduction axis, except that an indirect actuation similar to a SCS is used, with a belt replacing the cable however. The actuators and screw and nut systems are the same as on the flexion axes, but the primary belt differs in that it introduces a 2.33 reduction ratio, hence a force of 390N continuous and about 4600N peak in the nut. This force is equally distributed on the two abduction-adduction axes, whose movements are coupled using Delrin gears, through output pulleys whose neutral diameter equals 29mm, hence a theoretical continuous torque of 5.7Nm (peak torque 67Nm).

All four actuators are equipped with 1024ppt Maxon ENX16 magneto-optical encoders. Additional Megatron potentiometers are used to sense the rotation around the distal flexion axes.

3.3 Kinematics

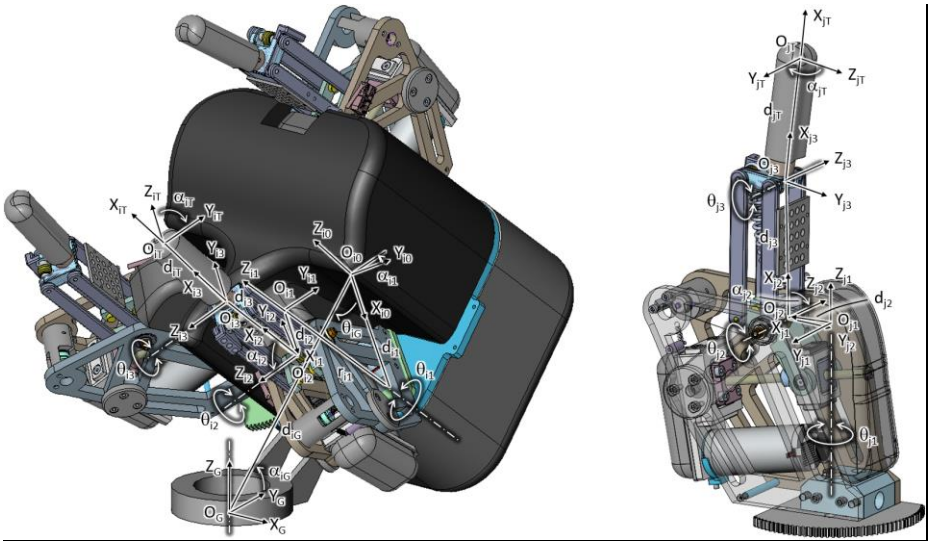

Fig. 3. Kinematics of the three fingers slave hand (left: complete gripper with index i used to describe the movable finger on the right, right: focus on the left finger labelled j).

The simplified kinematic model of the three fingers gripper is illustrated in Figure 3. It makes use of Denavit Hartenberg notations [23]. For each finger i, rotation θ_{i1} allows abduction-adduction, θ_{i2} proximal flexion and θ_{i3} distal flexion. A frame $R_{ik} = (O_{ik}, X_{ik}, Y_{ik}, Z_{ik})$ is first associated with each link k of finger i. By denoting d_{ik} (resp. α_{ik}) the distance from (resp. the angle between) $Z_{i\,k-1}$ to (and) Z_{ik} along axis $X_{i\,k-1}$ and r_{ik} and θ_{ik} the distance from (resp. the angle between) $X_{i\,k-1}$ to (and) X_{ik} along axis Z_{ik}, we can write the transformation matrix from $R_{i\,k-1}$ to R_{ik} as follows:

$$T_{i\,k-1\,k} = rot(X_{i\,k-1}, \alpha_{ik}).trans(X_{i\,k-1}, d_{ik}).rot(Z_{ik}, \theta_{ik}).trans(Z_{ik}, r_{ik}) \quad (1)$$

Additional frames $R_{iT} = (O_{iT}, X_{iT}, Y_{iT}, Z_{iT})$ are introduced at the tip of each finger i, so as to allow taking into account different lengths and shapes of the fingertips. By denoting d_{iT} the length of the distal phalanx, we have:

$$T_{i\,3T} = rot(X_{i3}, \alpha_{iT}).trans(X_{i3}, d_{iT}) \quad (2)$$

Finally, an additional frame $R_G = (O_G, X_G, Y_G, Z_G)$ is introduced at the base of the gripper (i.e. at level of the interface with the robot), allowing to express the configuration of the basis of all fingers in a common frame as follows:

$$T_{i\,G0} = rot(X_G, \alpha_{iG}).trans(Y_G, d_{iG}).rot(Z_{i0}, \theta_{iG}) \quad (3)$$

The transformation matrix of each finger can then be written:

$$T_{i\,GT} = T_{i\,G0}.T_{i\,01}.T_{i\,12}.T_{i\,23}.T_{i\,3T} \quad (4)$$

In practice θ_{i1} is obtained from the abduction-adduction sensors and θ_{i2} and θ_{i3} from the flexion sensors and the actuation and four bar mechanisms closed loop equations.

3.4 Manufacturing and integration

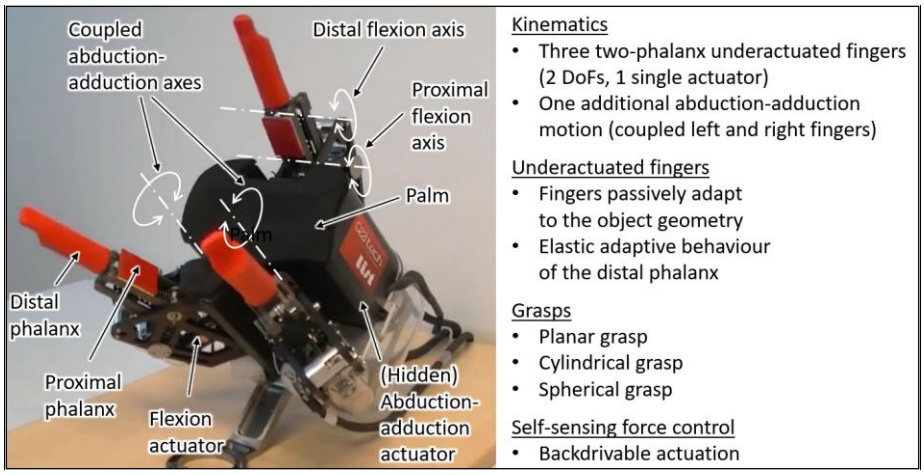

Fig. 4. CEA LIST's three fingers slave hand.

Figure 4 illustrates the prototype reconfigurable and under-actuated three-fingers robotic hand. The hand parts are made of aluminum and carbon fiber-reinforced plastics to remain as light as possible. All transmissions are placed inside the structural parts or covered with plastic shells in order to protect the mechanisms. Finally, the distal phalanges are covered with a soft polymeric envelope in order to increase grasping robustness when an object is held in hand, and a sharp end is provided in order to allow for

precision grasps. The controller comes in a separate box integrating 24V (for the sensors) and 48V (for the actuators) power supplies, Beckhoff analog input modules and Ethercat couplers and Maxon EPOS3 Ethercat drives.

As can be seen in figure 5, the range of motion of the different axes allow for the generation of planar, spherical and cylindrical grasps. In extreme configurations, the movable fingers point towards each other, or towards the third and fixed finger.

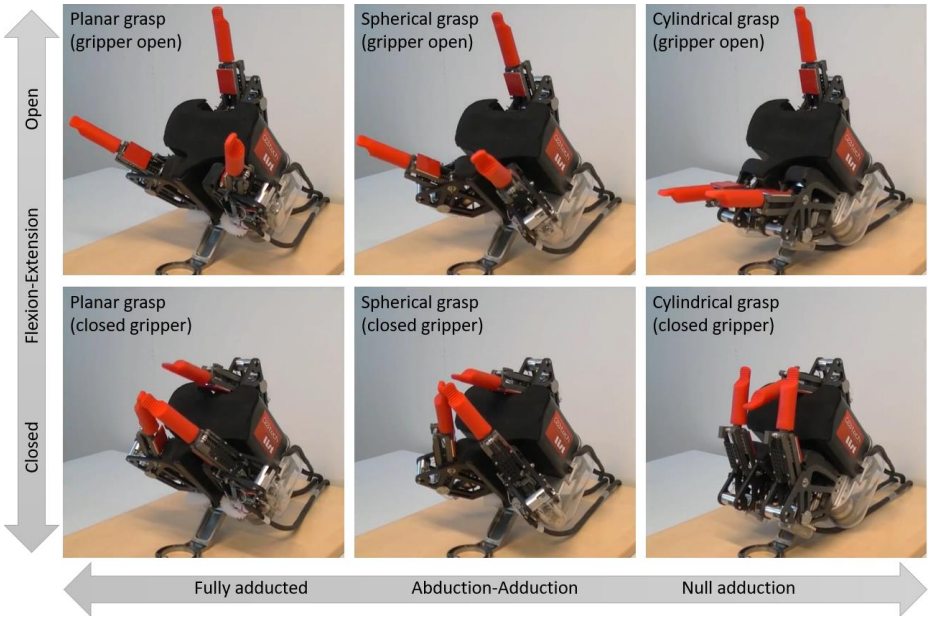

Fig. 5. CEA LIST's three fingers slave hand grasp types.

Such a three fingers design proves to be sufficient for coarse gripping and manipulating the to-be-sorted objects, yet it remains simple and rugged when compared to five-fingers hands which would be too fragile for such harsh environment. As shown in figure 6, it can generate power and precision grasp patterns [13], and it is capable of grasping a large variety of objects similar in size and weight to those encountered in nuclear waste containers.

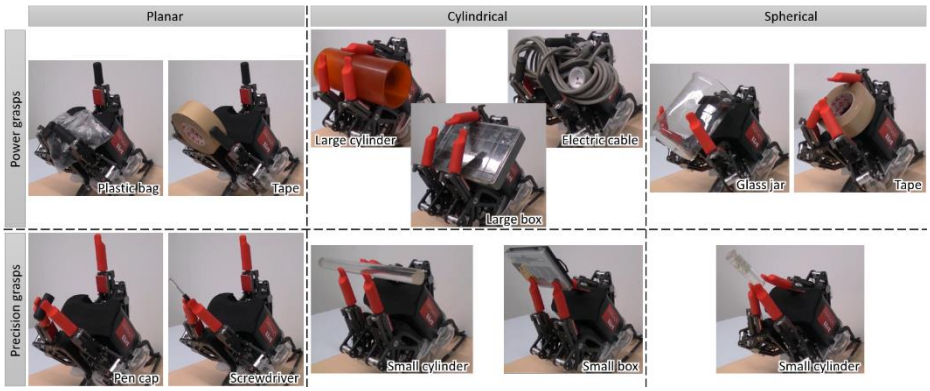

Fig. 6. Example grasps of representative objects as found in waste containers.

As can be seen in figure 7, during the course of the ROMANS project, the gripper was successively mounted on several robots thanks to its universal mechanical interface, among which a Yaskawa SIA10 (https://www.motoman.com/), an ABB IRB4600 (https://new.abb.com/) and a Stäubli RX160 (https://www.staubli.com/), for the purpose of integration, functional tests and controller tuning.

Fig. 7. Example set-ups on the slave side.

4 Tri-digital dexterous hand master

As mentioned in section 1, most teleoperated robots used to date in nuclear sites remain master-slave systems equipped with simple handles and grippers developed decades ago. Fortunately, huge progress has been obtained in the meantime in dexterous force feedback robotics and VR haptics. The requirement for anthropomorphic devices able to assist humans in force demanding applications (e.g. military, civil security, firemen, and even industry) or to restore lost motor abilities (e.g. rehabilitation, disabled people assistance), as well as the rise of Virtual Reality applications, led to the development of numerous arm and hand orthoses, exoskeletons and master devices [24] [25] [26] [27] [28]. The lessons learnt from these works were taken into account for the development of the tri-digital hand master presented in this section.

4.1 Design drivers

1/ Dexterous manipulation: the use of a tri-digital hand master appears as the most logical solution to control the three fingers slave hand. Interestingly, a more general study of manual interactions shows that three-fingers haptic devices offer a good compromise between manipulation capabilities and complexity [29]. As illustrated in figure 8, the percentage of our daily life activities that is possible when using two fingertips (pattern M3) is between 17.7 and 34.4% depending on the type of activities performed (rough manipulation, fine manipulation or manual exploration of the environment). It reaches 22.4 to 42.7% with three fingertips (pattern M4), 28.7 to 54.5% with four fingertips (pattern M5) and 33.3 to 61.7% with five fingertips (pattern M6). In theory, the more fingers you have the higher score you reach.

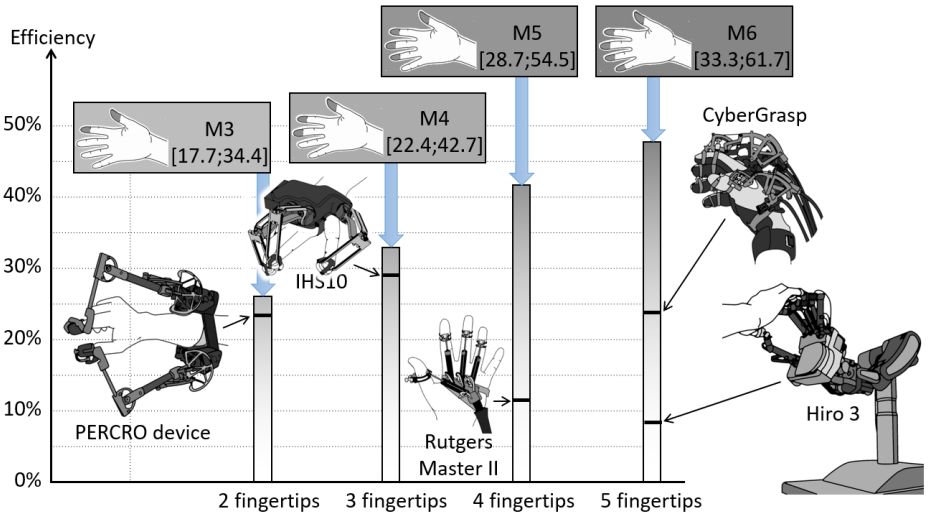

Fig. 8. Comparative study of the interaction efficiency of some existing fingertip input devices (figure adapted from [29]).

This is however not necessarily the case in practice as increasing the number of fingers the input device can track and apply force feedback on requires a higher number of DoFs, more links, joints and actuators. This added complexity tends to reduce the range of motion of the fingers, limit the force and stiffness available on each finger, increase friction and inertia, and globally limit the real efficiency. It appears indeed that, when taking into account all those criteria, the three fingers IHS10 glove [30] is more efficient than both the two fingers PERCRO device [31] and the four fingers Rutgers Master II [32] or the five fingers Cybergrasp [33] and Hiro 3 [34]. As a consequence, we will make use here of a three fingers device. In practice, this glove will be mounted at the tip of a Virtuose 6D and attached to the palm in order to allow for haptic feedback on both the palm and fingertips (this solution also allows compensating the glove's weight which has not to be carried on the hand).

2/ Universal fit: as explained in [35], two types of dexterous interfaces can be found in the literature. Exoskeletons, which are attached to every phalanges on which they can independently apply forces thanks to links and joints similar to the hand, allow simulating both precision and power grasps. They impose however hard mechanical constraints as their joints have to be roughly aligned with the fingers' ones. Hence, they must be tuned to each user, which is not convenient for a universal device that can be used by different operators. On the contrary, fingertip interfaces are fixed only on the palm and distal phalanges, and their geometry is less restricted, making them easily usable by different users. Their design is also much simpler. These advantages led us to focus on fingertip devices. To allow for natural interactions with the palm and fingers, links and joints have to be positioned and dimensioned so that the robot does not limit the fingers' movements.

3/ High transparency and force feedback quality: haptic interfaces should be transparent in free space, i.e. display a mechanical impedance that is sufficiently low for the user to forget their presence. They should also be able to provide high impedances to simulate realistic contacts with stiff surfaces. This contradiction usually leads to a compromise between a high transparency in free space (i.e. low friction and inertia) and realistic force feedback in contact (i.e. high forces and stiffness). Here, we will exploit the fact that the slave hand has only one actuator per finger to control it with a glove having also only one actuator per finger, allowing to greatly simplify the design and favor a high transparency.

4.2 Electro-mechanical design

The tri-digital master glove is illustrated in figure 9. It is composed of a base plate fixed on the palm and 3 robots allowing to track and apply forces on the distal phalanx of the thumb, index and middle finger to which they are attached. The base is dimensioned so that the index and middle robots' abduction-adduction axes best align with the fingers' ones (they are theoretically aligned for an adult man corresponding to the 50^{th} percentile of the population).

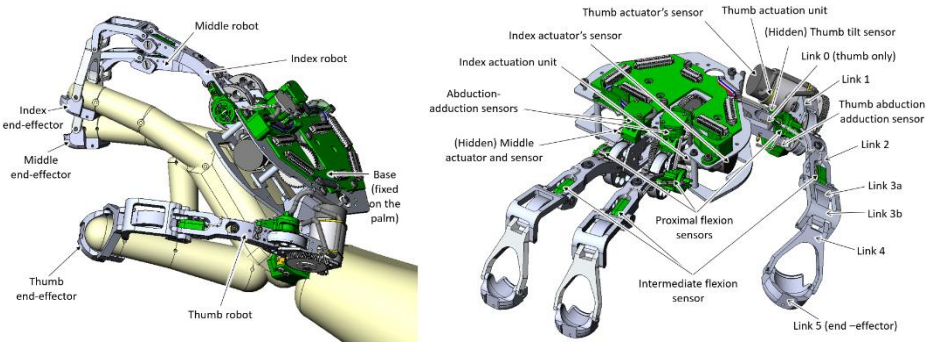

Fig. 9. Overview and main components of the tri-digital master glove (figure adapted from [8]).

Each robot is composed of 6 links (7 for the thumb, owing the requirement to make thumb opposition), allowing to move the fingers freely in their entire workspace. Joint sensors are integrated in the abduction-adduction, proximal flexion and intermediate flexion axes, as well as on the tilt axis of the thumb, allowing to compute the end-effectors' positions in space. Each robot is provided with a single actuation unit enabling force feedback at the fingertips roughly normal to the finger pulp (see figure 10). These actuators are equipped with high resolution incremental encoders, ensuring high quality position control. The design of the base plate, links dimensions and joints' range of motion were optimized in order to allow free movements of the fingers over their entire workspace. It is worth mentioning that, unlike gloves and exoskeletons whose dimensions fit specific users, fingertip devices can accommodate different hand sizes. Our device, whose design was inspired by the dexterous interface with hybrid haptic feedback for Virtual Reality applications presented in [35], can therefore easily be used by various users.

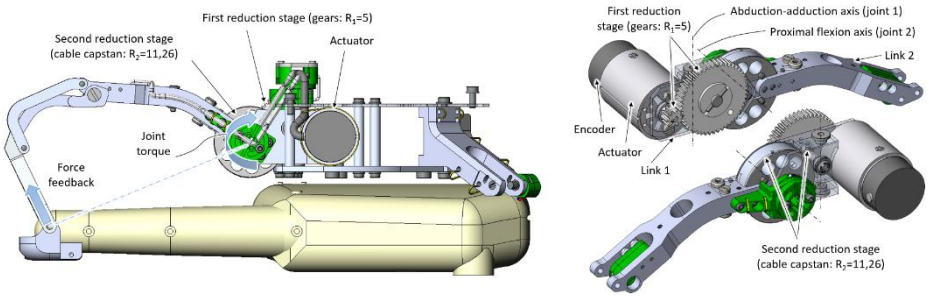

Fig. 10. Force feedback generated on fingertips and actuation units (figure adapted from [8]).

As shown in figure 10, force feedback is obtained with a Maxon REmax21 221028 DC motor (12V, continuous torque 6.07mNm, peak torque 17.3mNm [21]) associated with a two stages reducer combining:

- A gear reducer with Delrin gears of 0.5 modulus allowing to obtain a reduction ratio of 5 (10 teeth primary gear HPC ZG0.5-10 glued on the motor axis, 50 teeth secondary gear HPC ZG0.5-50 as output).
- A miniature cable capstan reducer making use of a Berkley Whiplash Pro 0.42mm Dyneema cable attached to pulleys of diameter 2.3mm and 25.9mm, hence a ratio of 11.26.

Such combination is highly transparent and backdriveable, yet compact and light. It ensures that, even if backlash occurs in the gear reducer, its amplitude is downscaled at the output of the cable capstan reducer, making if almost negligible in practice. It allows generating a continuous joint torque equal to 0.342Nm and a peak joint torque of 0.974Nm on the proximal flexion joint. This torque generates a force on the distal phalanx whose amplitude and direction depend on the finger configuration. Force is almost normal to the pulp when the finger is straight. The distance between the actuated axis and the fingertip being about 78.8mm in this configuration for an adult man of medium size, continuous force is equal to 4.3N and peak force to 12.4N.

The motors are equipped with 512ppt (2048ppt after interpolation) magneto-optical encoders (ref. Maxon MR 201940). 1024ppt Hall effect sensors are added at the joint level on the abduction-adduction axis and on the proximal and intermediate flexion axes (ref. sensors RLS RM08 VB 00 10 B02 L2 G00, ref. magnets RMM44 A3 A00). One can notice that the measurement of the proximal flexion is redundant. It is worth noting that both sensors are however not used for the same purposes.

- Owing the reduction ratio, the motor encoders give a very precise information, and they are co-located with the actuators. They are used for the position and force control (master and slave hands are linked using a bilateral position coupling scheme). However, these sensors do not allow to know the system configuration at start-up (these sensors are incremental).
- The role of the joint sensors is precisely to give an absolute joint angle value, avoiding the need for initialization when the glove is turned on.

4.3 Kinematics

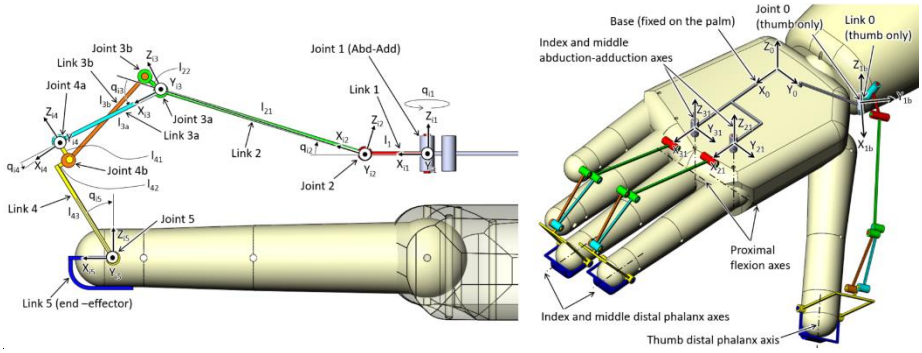

Fig. 11. Kinematic model of the master glove. A frame $R_{ik} = (O_{ik}, X_{ik}, Y_{ik}, Z_{ik})$ is associated with each link k of finger i, with i=1 for the thumb, i=2 for the index and i=3 for the middle finger, with its origin positioned on the joint axis. q_{ik} is the rotation around joint k of finger i, and l_k (resp. l_{k1}, l_{k2}, l_{k3}) designates the length of link k (resp. of different parts of link k). An additional frame $R_{1b} = (O_{1b}, X_{1b}, Y_{1b}, Z_{1b})$ is introduced for the thumb which has an extra joint (figure adapted from [8]).

The simplified kinematic model of the master glove is illustrated in figure 11. Link 1 allows abduction-adduction while the other links allow finger flexion-extension. The links 2, 3a, 3b and 4 form an inverted parallelogram which allows the robot to remain close to the finger in its entire workspace. A pivot joint is added at the end of this structure to allow for the fingertip to rotate freely when the operator closes the hand.

It is worth noting that, contrary to the slave hand which comes from the field of robotics and for which we use Denavit Hartenberg (DH) conventions, the master hand device's design is inspired from the haptic glove presented in [35] which is used in Virtual Reality applications in which DH parameters are rarely used. In practice, we use the more simple notations given in figure 11, with which the kinematic model of

the thumb, index and middle robots can be written as follows (with i=1 for the thumb, i=2 for the index and i=3 for the middle finger):

$$T_{i\,01} = \text{trans}(X_0, d_{ix}).\text{trans}(Y_0, d_{iy}).\text{rot}(Z_0, q_{i1}) \quad (5)$$

$$T_{i\,12} = \text{trans}(X_{i1}, l_1).\text{rot}(Y_{i1}, q_{i2}) \quad (6)$$

$$T_{i\,23} = \text{trans}(X_{i2}, l_{21}).\text{rot}(Y_{i2}, q_{i3}) \quad (7)$$

$$T_{i\,34} = \text{trans}(X_{i3}, l_{3a}).\text{rot}(Y_{i3}, q_{i4}) \quad (8)$$

$$T_{i\,45} = \text{trans}(Z_{i4}, -l_{41}-l_{43}).\text{trans}(X_{i4}, l_{42}).\text{rot}(Y_{i4}, q_{i5}) \quad (9)$$

For the thumb, equation (1) is replaced with the following equations:

$$T_{1\,b0} = \text{trans}(X_0, d_{1x}).\text{trans}(Y_0, d_{1y}).\text{trans}(Z_0, d_{1z}).\text{rot}(Z_0, q_{1z0}).\text{rot}(X_{1b}, q_{1x0}) \quad (10)$$

$$T_{1\,01} = \text{trans}(Z_{10}, l_0).\text{rot}(Z_{10}, q_{11}) \quad (11)$$

In these equations, q_{i1}, q_{i2} and q_{i3} are given by the motors' and joints' sensors, while q_{i4} can be computed from q_{i3} by solving the equations of the inverted parallelogram as explained in [35] and [36]. The distal rotation q_{i5} is not measured nor computed as the position of the fingertip, which is the information of interest, does not depend on it.

4.4 Manufacturing and integration

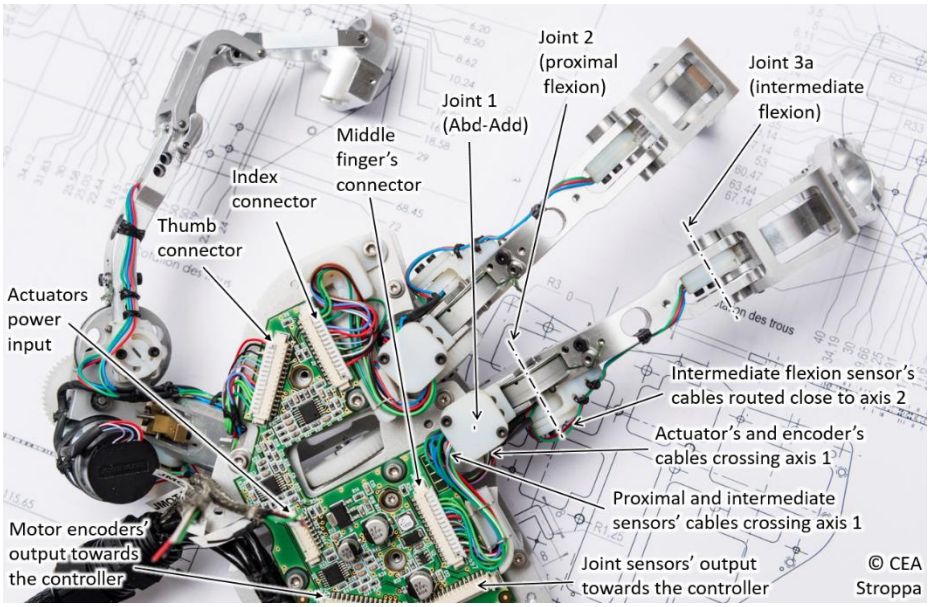

Fig. 12. Main components and cabling of the manufactured dexterous hand master prototype.

The manufactured prototype made of aluminum parts and its main components are shown in figure 12. A specific attention was given to the routing of the actuators and sensors cables which are guided along the robots' structure so that they pass the closest possible to the joints' axes in order to resist as less as possible to the links' movements. A custom designed PCB, integrated in the base plate, is used to connect the glove to its controller. This PCB is in charge of both powering the sensors and actuators and of conditioning and filtering the sensors' signals. In order to favor modularity, each finger is connected to this PCB through a specific connector on the robots' side, and three connectors are used on the controller side, respectively in charge of the actuators power supply, motors' encoders and joint sensors. As shown in figure 13, this PCB is protected by a thin plastic part, and the base is attached to a mitten through a 3D printed part. This way, the glove can be easily put on or taken off.

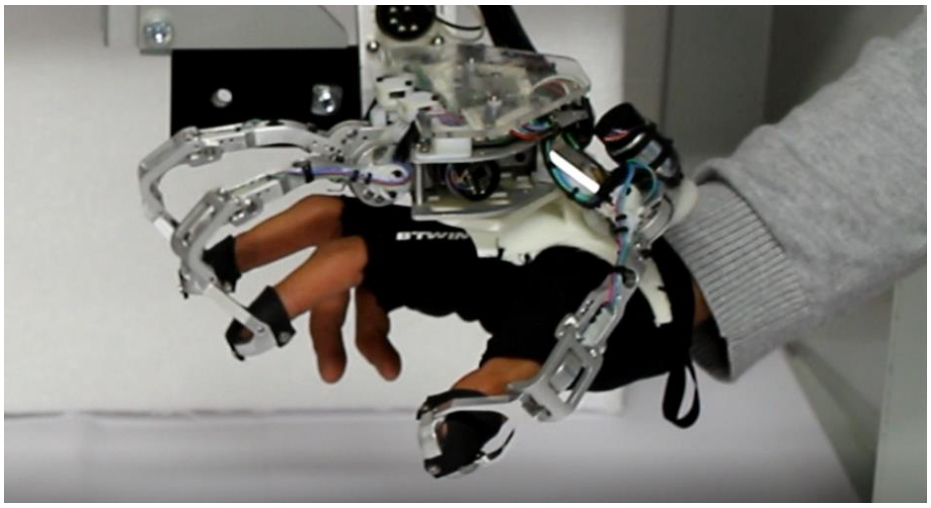

Fig. 13. Fully integrated dexterous master glove (source [8]).

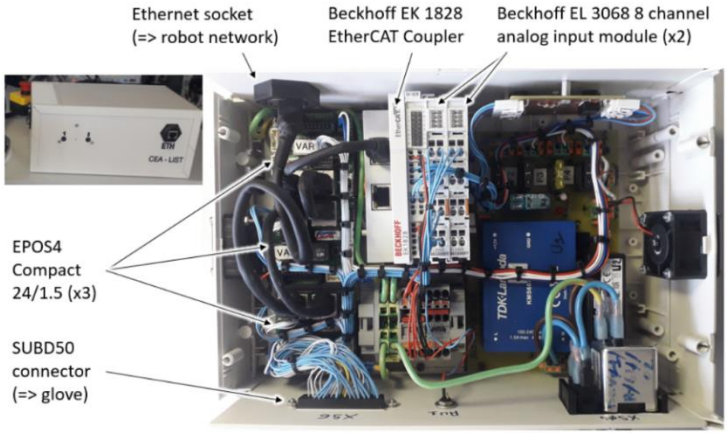

Fig. 14. Dexterous hand master controller (source [8]).

The haptic master glove is controlled using an Ethercat controller illustrated in Figure 14. Three Maxon EPOS4 Compact 24/1.5 modules are used for controlling the actuators, while a Beckhoff EK1828 Ethercat Coupler connected to two Beckhoff EL 3068 analog input modules with 8 channels each (0-10V, 12 bits) is used to connect the joint sensors. The controller also integrates 12V (for the EPOS4 modules) and 24V (for the Beckhoff modules and the glove PCB) power supplies. It is connected to the glove through a SUBD 50 connector and to the robot through an Ethernet socket.

5 Bi-manual teleoperation controller

5.1 Detailed presentation of the bi-manual teleoperation set-up

As previously stated, our bi-manual teleoperation platform is composed of two robots on the slave side, a Stäubli RX160 equipped with the three fingers gripper and a prototype Isybot cobot (https://www.isybot.com/) provided with a bi-digital gripper with parallel jaws both developed at CEA LIST (see figure 15). This configuration allows efficiently performing dexterous operations with both hand, as human naturally do in everyday life, either to move an object with both hands or to hold it with one hand while making an operation on it with the other hand.

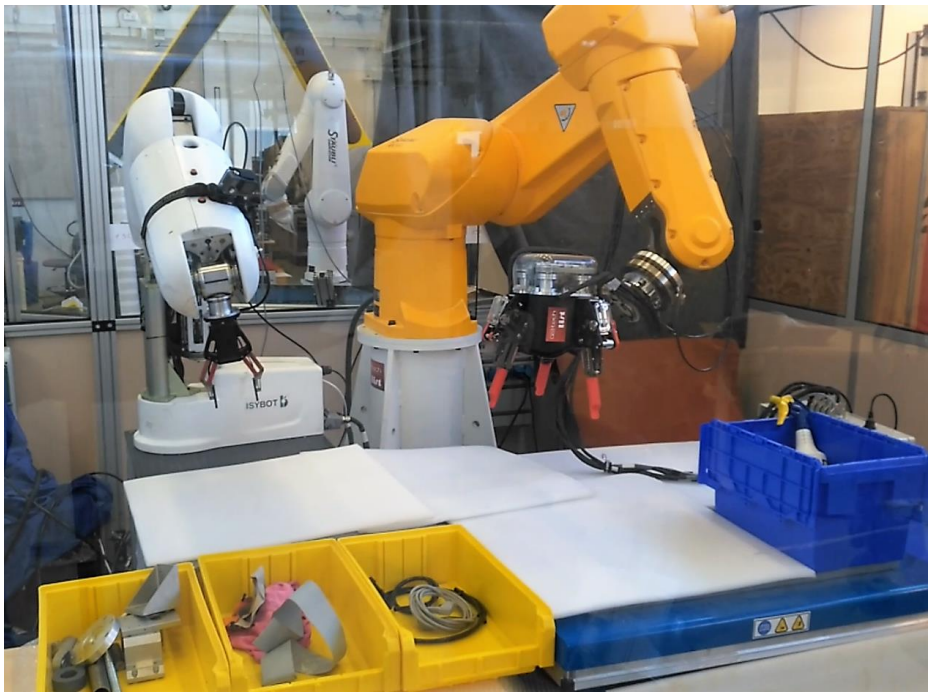

Fig. 15. Slave side of the bi-manual dexterous teleoperation platform.

All CEA devices (i.e. all but the RX160) make use of ball screw reducers. They come with direct transmissions on the three digital gripper as presented above and on the second robot pair of pliers with parallel jaws whose design will not be detailed here, and with a secondary cable transmission as presented in [22] on the prototype cobot whose design will neither be presented here. This particular type of reducers and transmissions are key innovative elements enabling these robot and grippers to have a very high level of mechanical transparency (i.e. very low friction and inertia) and back-drivability. This solution provides accurate joint torque estimates from simple current sensing, without the need for delicate electronic sensors which would fail in high beta and gamma radiation environments as encountered on nuclear sites. Note that current sensing is also used in conventional robot arms to provide torque estimates, but these measurements are significantly erroneous due to the higher inertia and friction of conventional actuators. As a consequence, the RX160 is equipped with an ATI 6 DoF force/torque sensor placed between its end-effector and the gripper, allowing a direct measure of the efforts applied on the robot. When moving to a real environment, this sensor will have to be replaced with a radiation hardened sensor with a remote electronics as in [3].

Fig. 16. Master side of the bi-manual dexterous teleoperation platform.

As shown in figure 16, these robots are controlled using two input devices mapping the slave-arm capabilities. A Virtuose 6D TAO master arm from Haption is used to control the Isybot prototype with 6DoF force feedback. This input device is further equipped with an instrumented handle which enables a fine control of the gripper's closing and opening movement. A second Virtuose 6D TAO is used to control the Stäubli RX160.

It is worth noting that the Virtuose is provided with a universal handle adapter, allowing to easily shift from one handle to another. The original handle is replaced here with our novel tri-digital master glove, allowing fine control of the dexterous gripper with force feedback on both the palm and fingers. This set-up is intended to enable high fidelity dexterous force-reflection tele-presence.

5.2 Master-slave coupling

Our bi-manual teleoperation platform is controlled using the TAO framework. TAO is a teleoperation middleware allowing a high-speed synchronization and control of several real or virtual mechanisms (e.g. master arms, slave arms, dynamic simulators) [4]. Among the different TAO teleoperation modes, we make use here of master-slave bilateral position coupling schemes as they provide a compelling force feedback yet prove to be passive (i.e. stable whatever the actions of the human operator and the efforts applied on the slave robots) when the control gains are properly tuned.

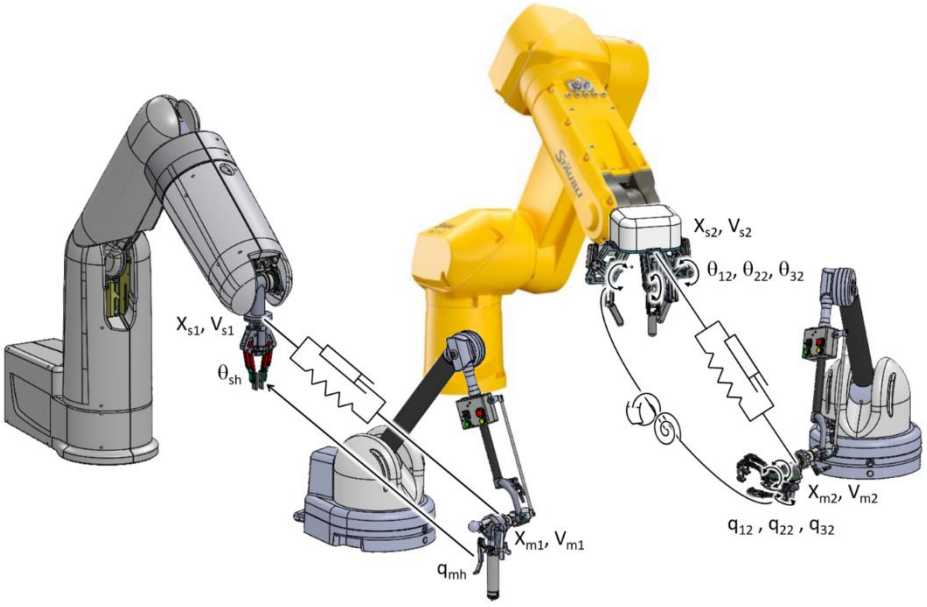

Fig. 17. Master-slave coupling schemes of the bi-manual dexterous teleoperation platform.

As shown in figure 17, different implementations of this bilateral position couplings are used in practice:

- The Isybot prototype and the associated Virtuose 6D master arm, as well as the Stäubli RX160 and the second Virtuose 6D, are coupled in the Cartesian space as they have different kinematics. Denoting X_{s1} and X_{s2}, respectively X_{m1} and X_{m2}, the configuration of their end-effector, respectively of their handle, computed from their joint measurements using their direct geometric model, and V_{s1}, V_{s2}, V_{m1} and V_{m2}

their kinematic twists evaluated with their Jacobian matrix $J_{si}(\theta_i)$ (respectively $J_{mi}(q_i)$) expressed in the base frame and reduced to the center of the end-effector, we can write these coupling schemes as follows:

$$F_{si} = -H_f.F_{mi} = K.(X_{mi} - H_p.X_{si}) + B.(V_{mi} - H_p.V_{si}) \quad (12)$$

With : K the position control gain expressed in N/m and Nm/rad (K is usually represented as a spring, as shown in figure 17).
B the speed gain expressed in N/m/s and Nm/rad/s (B is usually represented as a damper).
H_p an optional position scaling factor ensuring a multiplied movement on the slave side compared to the master side (the master movements are H_p times larger than the slave ones).
H_f an optional force and torque scaling factor allowing the slave arms to produce efforts H_f times larger than the forces applied on the master arm.

The torques applied on the different joints of the master and slave arms to ensure these coupling are then computed as follows:

$$\tau_{mi} = J_{mi}^T(q_i).F_{mi} \quad (13)$$

$$\tau_{si} = J_{si}^T(\theta_i).F_{si} \quad (14)$$

It is worth noting that the scaling factors are very convenient when the master and slave arms have different workspaces and/or force and torque capacities. They should however be used with care as they introduce several changes in the stimuli perceived by the human operator.

First, a large position scaling factor allows large slave displacements with limited hand movements, hence reducing fatigue, but small and precise slave movements become very difficult as every single small hand displacement is amplified and produces a large slave movement. Fortunately, the TAO framework also implements a software clutch function, i.e. the master and slave arm are coupled only if the clutch is engaged, and they can move independently when it is disengaged. In practice, it is possible to control the slave robots by moving the master arms as long as the handle remain in an ergonomic and comfortable volume, and to disengage the clutch as soon as their configuration is no more convenient, then to move back the master arms in more comfortable configurations and re-engage the clutch to continue working. This way, the slave robots can span a much larger volume than the master arms without the need for large position scaling factors. In practice, the position scaling factor were kept equal to 1 here.

The same is true for the force scaling factors. Large scaling reduces fatigue but diminishes the user sensitivity. Also, if the position and force scaling factors differ, the perceived environment dynamics will be modified (e.g. with a position factor of 1, i.e. the master and slave move the same amplitude, and a force factor of 2, i.e. the slave applies two times more force than the master, the user will perceive the contacted objects as two times softer as half the same force will produce the same movement). In practice, force scaling factors were kept low, i.e. equal to 1.

- As the three fingers slave hand and the tri-digital hand master are underactuated, it is not possible to couple them in Cartesian space. They are coupled in joint space instead and their behavior is the governed by the following equation:

$$\tau_{si2} = -h_f.\ \tau_{mi2} = k.(q_{i2} - h_p.\theta_{i2}) + b.(\dot{q}_{i2} - h_p.\ \dot{\theta}_{i2}) \quad (15)$$

With : τ_{si2} (respectively τ_{mi2}) the joint torques applied on the second axis of the finger i of the slave hand (respectively the master hand device).
k the joint position control gain expressed in Nm/rad.
b the joint speed gain expressed in Nm/rad/s.
h_p an optional joint position scaling factor.
h_f an optional joint torque scaling factor.
q_{i2} (respectively $\dot{q}_{i2}$) the joint position (respectively the joint speed) of the second joint (i.e. the actuated joint) of the i^{th} finger of the tri-digital master hand device (see figure 11).
θ_{i2} (respectively $\dot{\theta}_{i2}$) the joint position (respectively the joint speed) of the second joint (i.e. the actuated joint) of the i^{th} finger of the three fingers slave hand (see figure 3).

In practice, the position scaling factors were tuned so that the slave hand closes completely when moving the master hand. The force required to grasp the large and heavy objects encountered in our use-case being much higher than the human hand grasping forces, themselves higher than the master hand torques, a 1/10 force scaling factor (i.e. the maximum value allowed by TAO) was used to couple the master and slave hands.

- As the instrumented handle of the Virtuose 6D is not actuated, it is not possible to provide force feedback on the left hand grasping movement and the bi-digital gripper's opening movement θ_{sh} is controlled in position in open loop so as to follow the handle movement q_{mh}.

5.3 Tri-digital master-three fingers slave hand mapping

As previously stated, the master hand-slave hand coupling is performed using a bilateral position coupling scheme implemented in the joint space. This solution was chosen to keep the coupling as intuitive as possible for the user, so as to limit his or her cognitive load.

In practice however, it is difficult to control the slave hand intuitively if the master fingers are always coupled with the same slave fingers as the slave hand can have configurations that largely differ from the human hand. If for example we couple the thumb with the fixed slave finger and the index and middle with the moving fingers, the slave hand behavior will be natural for cylindrical grasps as the slave 'thumb' will face the other two fingers. The spherical grasps will also be quite natural as the slave fingers will encompass the object just as the user fingers would do in direct manipulation. The planar grasps will however not be natural at all, as the fingers controlling the slave hand's closing and opening movement will be the index and middle fingers while one would expect planar grasps to occur between the thumb and the index or middle. And

the same limitations appear whatever the choice of fixed master-slave fingers association. To cope with this issue, we developed an adaptive mapping strategy allowing to keep natural master hand glove configurations whatever the type of grasp performed by the slave hand. With respect to figure 18, the principle is the following:

- In planar grasps, only the moving fingers of the slave hand (i.e. fingers A and C) are active and involved in the coupling (finger B is blocked in open position). The thumb and index are coupled with fingers A and C (the middle is not used).
- In spherical grasps, the thumb is coupled with finger A, the index with finger B and the middle finger with finger C.
- Finally, in cylindrical grasps, finger A and C have to move in the same manner in order to ensure a correct closure. To meet this requirement, the thumb is coupled with finger A and the index with finger B. Then finger C is coupled with finger A, and the middle is coupled to finger C. This way, fingers A and C move similarly, as well as the thumb and the middle fingers.

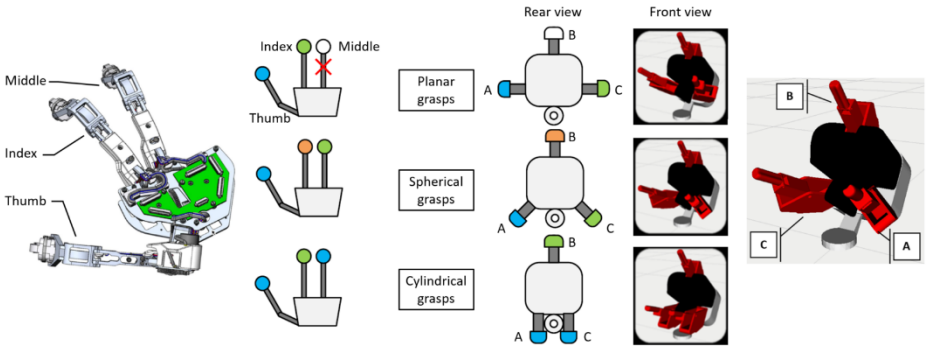

Fig. 18. Master and slave fingers mapping.

In practice, the change from one grasp to another is managed by a state machine. It was first tested to use the master thumb abduction-adduction imposed by the operator's hand to choose the grasp type and then to maintain it until the object is fully grasped. It appeared however that using a simple external selector is more comfortable to switch the abduction configuration between three main positions.

First tests consisted in verifying that the slave hand can be controlled by moving the master glove, and reversely that the master hand reproduces the slave hand's motions (see figure 19). Then the master glove was used to remotely grasp various object with force feedback (see figure 20).

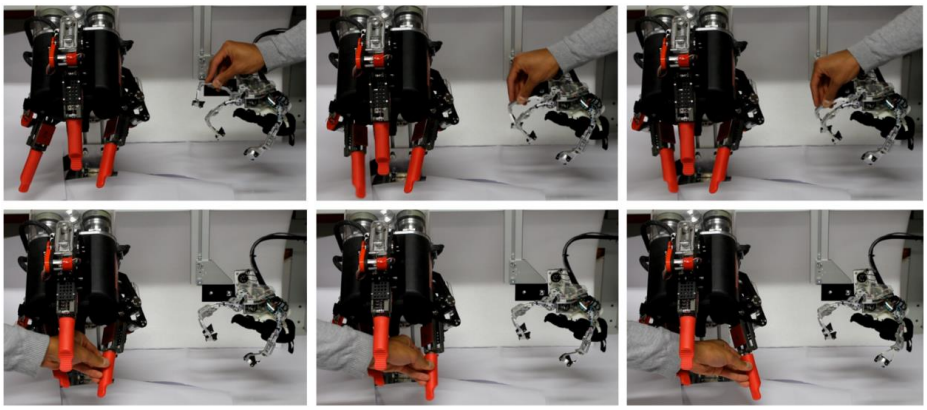

Fig. 19. Functional validation of the bilateral joint position coupling scheme. Top: direct sense (from the master middle to the slave). Bottom: inverse sense (from the slave to the master thumb).

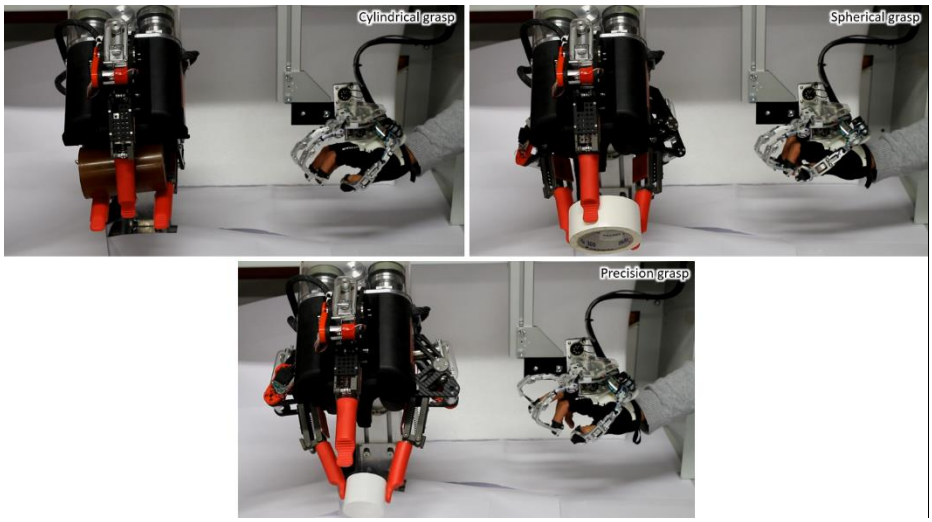

Fig. 20. Functional validation of teleoperated cylindrical, spherical and planar grasps (adapted from [8]).

6 Bi-manual teleoperation tests and validation

Once validated, the master hand glove was mounted on a Virtuose 6D master arm, and it was further associated with a second master slave system. The resulting bi-manual teleoperation setup was used to test the ability of an operator to grasp and manipulate several types of objects similar to the waste found in nuclear containers (e.g. piece of cloth, rigid objects, cables, etc.). As shown in figure 21, these operations were successful. It was even possible to pass objects from one robot to the other.

Fig. 21. Grasping various objects in bi-manual teleoperation (adapted from [8]).

7 Conclusions and perspectives

This paper presents a novel bi-manual dexterous teleoperation setup for nuclear waste remote manipulation. This platform is composed of an underactuated three fingers slave gripper mounted on a large capacity slave robot and a simple bi-digital gripper with parallel jaws fixed on a cobot prototype. These slave robots are controlled using two Virtuose 6D TAO master arms, one of which is equipped with a novel tri-digital master hand device. Master and slave robots are coupled using a bilateral position coupling scheme implemented in the Cartesian space for the robots and in the joint space for the hands, with a mapping strategy allowing to intuitively control cylindrical, spherical and planar grasps. This system proves to be able to grasp various objects similar in size and shape as those encountered in waste containers. The operator is able to extract the objects, pass them from one robot to the other and sort them in various deposit boxes. This functional tests validate the ability of this system to perform nuclear sort and segregation tasks. Future work should be dedicated to a more precise experimental characterization of the platform performances.

Acknowledgments. The authors would like to thank the colleagues who contributed to the technical developments presented in this article, especially D. Diallo, B. Perochon and P. Chambaud. This research was partly supported by the Horizon 2020 RoMaNS project (Robotic Manipulation for Nuclear Sort and Segregation, #645582) funded by the European Commission.

References

1. Köhler, G.W.: Typenbuch der Manipulatoren - Manipulator type book. Thiemig Taschenbücher, Verlag Karl Thiemig, München, Germany (1981).
2. Vertut, J., Coiffet, P.: Les robots - Tome 3A : téléopération, évolution des technologies. Hermès Publishing, Paris, France (1984).
3. Piolain, G., Geffard, F., Coudray, A., Garrec, P., Thro, J.F., Perrot, Y.: Dedicated and Standard Industrial Robots used as Force-Feedback Telemaintenance Remote Devices at the AREVA Recycling Plant. In: Proc. 1st IEEE Int. Conf. on Applied Robotics for the Power Industry, pp. 1-6, Montreal, QC, Canada (2010)
4. Geffard, F., Garrec, P., Piolain, G., Brudieu, M.A., Thro, J.F., Coudray, A., Lelann, E.: TAO2000 V2 Computer-Assisted Force Feedback Telemanipulators Used as Maintenance and Production Tools at the AREVA NC-La Hague Fuel Recycling Plant. Journal of Field Robotics 29(1), 161-174 (2012).
5. European Commission Portal, Robotic Manipulation for Nuclear Sort and Segregation (ROMANS), https://cordis.europa.eu/project/id/645582, last accessed 2022/03/02.
6. World Nuclear News, Funding for waste-handling robotics development, https://www.world-nuclear-news.org/NN-Funding-for-waste-handling-robotics-development-2502154.html, last accessed 2022/03/02.
7. Marturi, N., Rastegarpanah, A., Takahashi, C., Adjigble, M. Stolkin, ,R., Zurek, S., Kopicki, M., Talha, M., Kuo, J.A., Bekiroglu, Y.: Towards advanced robotic manipulation for nuclear decommissioning: a pilot study on tele-operation and autonomy. In: Proc. Int. Conf. on Robotics and Autom. Humanitarian Applications, 8p, Amritapuri, India (2016).
8. Gosselin, F., Grossard, M., Diallo, D., Perochon, B., Chambaud, P.: Design and Development of a Dexterous Master Glove for Nuclear Waste Telemanipulation. In: Proc. 18th Int. Conf. on Informatics in Control, Autom. and Robotics, pp. 459-468, Online (2021).
9. Kochan, A.: Shadow delivers first hand. Industrial Robot: an Int. Journal 32(21), 15-16 (2005).
10. Walker, R., De La Rosa, A., Elias, H., Godden, M., Goldsmith, J.: Advances in Actuation Technology for Compliant Dextrous Manipulation. In: Proc. IEEE Int. Conf. on Robotics and Biomimetics, pp. 1429-1433, Tianjin, China (2010).
11. Martin Amezaga, J., Grossard, M.: Design of a Fully Modular and Backdriveable Dexterous Hand. The Int. Journal of Robotics Research 33(5), 783-798 (2014).
12. Grebenstein, M., Albu-Schäffer, A., Bahls, T., Chalon, M., Eiberger, O., Friedl, W., Gruber, R., Haddadin, S., Hagn, U., Haslinger, R., Höppner, H., Jörg, S., Nickl, M., Nothhelfer, A., Petit, F., Reill, J., Seitz, N., Wimböck, T., Wolf, S., Wüsthoff, T., Hirzinger, G.: The DLR Hand Arm System. In: Proc. IEEE Int. Conf. on Robotics and Automation, pp. 3175-3182, Shanghai, China (2011).
13. Cutkosky, M.R.: On grasp choice, grasp models, and the design of hands for manufacturing tasks. IEEE Trans. on Robotics and Automation 5(3), 269–279 (1989).
14. Feix, T., Pawlik, R., Schmiedmayer, H.B., Romero, J., Kragic, D.: A Comprehensive Grasp Taxonomy. In: Robotics, Science and Systems Conf.: Workshop on Understanding Human Hand for Advancing Robotic Manipulation, pp. 58-59, Seattle, WA, USA (2009).
15. Fishel, J.A., Oliver, T., Eichermueller, M., Barbieri, G., Fowler, E., Hartikainen, T., Moss, L., Walker, R.: Tactile Telerobots for Dull, Dirty, Dangerous, and Inaccessible Tasks. In: Proc. IEEE Int. Conf. on Robotics and Autom., pp. 11305-11310, Paris, France (2020).
16. Mnyusiwalla, H., Vulliez, P., Gazeau, J.P., Zeghloul, S.: A New Dexterous Hand Based on Bio-Inspired Finger Design for Inside-Hand Manipulation. IEEE Trans. on Systems, Man and Cybernetics 46 (6), 809-817 (2016).

17. Yuan, S., Epps, A.D., Nowak, J.B., Salisbury, J.K.: Design of a Roller-Based Dexterous Hand for Object Grasping and Within-Hand Manipulation. In: Proc. IEEE Int. Conf. on Robotics and Automation, pp. 8870-8876, Paris, France (2020).
18. Townsend, W.: The BarrettHand grasper - programmably flexible part handling and assembly. Industrial Robot: An International Journal 27(3), 181-188 (2000).
19. Birglen, L., Gosselin, C.M.: Kinetostatic Analysis of Underactuated Fingers. IEEE Trans. on Robotics and Automation 20(2), 211-221 (2004).
20. Birglen, L., Laliberté, T., Gosselin, C.: Underactuated Robotic Hands. Springer Tracts in Advanced Robotics 40, Springer-Verlag, Berlin-Heidelberg, Germany (2008).
21. Maxon : Maxon motor catalogue, programme 2016-2017 (2016).
22. Garrec, P.: Screw and cable actutators (SCS) and their applications to force feedback teleoperation, exoskeleton and anthropo-morphic robotics. In: Robotics 2010: Current and Future Challenges, pp. 167-191, Intech: Rijeka, Croatia (2010).
23. Khalil, W., Dombre, E. : Modélisation, identification et commande des robots, 2nd edition. Hermès Science Publications, Paris, France (1999).
24. Bogue, R.: Exoskeletons and robotic prosthetics: a review of recent developments. Industrial Robot: An International Journal 36(5), 421-427 (2009).
25. Foumashi, M.M., Troncossi, M., Parenti Castelli, V.: State of the-art of hand exoskeleton systems. Internal report, Univ. Bologna, 54p (2011).
26. Heo, P., Min Gu, G., Lee, S.J., Rhee, K., Kim, J.: Current Hand Exoskeleton Technologies for Rehabilitation and Assistive Engineering. Int. J. Precision Engineering and Manufacturing 13(5), 807-824 (2012).
27. Gopura, R.A.R.C., Bandara, D.S.V., Kiguchi, K., Mann, G.K.I.: Developments in hardware systems of active upper-limb exoskeleton robots: A review. Robotics and Autonomous Systems 75(B), 203-220 (2016).
28. Perret, J., Van der Poorten, E.: Touching Virtual Reality: A Review of Haptic Gloves. In: Proc. 16th Int. Conf. on New Actuators, pp. 270-274, Bremen, Germany (2018).
29. Gonzalez, F., Gosselin, F., Bachta, W.: Analysis of Hand Contact Areas and Interaction Capabilities During Manipulation and Exploration. IEEE Trans. on Haptics 7(4), 415-429 (2014).
30. Gosselin, F.: Guidelines for the design of multi-finger haptic interfaces for the hand. In: Proc. 19th CISM-IFToMM Symp. on Robot Design, Dynamics and Control, pp. 167–174, Paris, France (2012).
31. Frisoli, A., Simoncini, F., Bergamasco, M., Salsedo, F.: Kinematic design of a two contact points haptic interface for the thumb and index fingers of the hand. ASME Journal of Mechanical Design 129(5), 520–529 (2007).
32. Bouzit, M., Burdea, G., Popescu, G., Boian, R.: The Rutgers master II—New design force-feedback glove. IEEE/ASME Trans. on Mechatronics 7(2), 256–263 (2002).
33. Aiple, M., Schiele, A.: Pushing the limits of the CyberGraspTM for haptic rendering. In: Proc. IEEE Int. Conf. on Robotics & Autom., pp. 3541–3546, Karlsruhe, Germany (2013).
34. Endo, T., Kawasaki, H., Mouri, T., Ishigure, Y., Shimomura, H., Matsamura, M., Koketsu, K., Five-fingered haptic interface robot: HIRO III. IEEE Trans. in Haptics 4(1), 14–27 (2011).
35. Gosselin, F., Andriot, C., Keith, F., Louveau, F., Briantais, G., Chambaud, P.: Design and Integration of a Dexterous Interface with Hybrid Haptic Feedback. In: Proc. 17th Int. Conf. on Informatics in Control, Automation and Robotics, pp. 455-463, Online (2020).
36. Ngalé Haulin, E., Lakis, A.A., Vinet, R.: Optimal synthesis of a planar four-link mechanism used in a hand prosthesis. Mechanism and Machine Theory 36(11-12), 1203-1214 (2001).